

## Status of the NICA project at JINR

V. Kekelidze<sup>1,a</sup>, A. Kovalenko<sup>1</sup>, R. Lednicky<sup>1</sup>, V. Matveev<sup>1</sup>, I. Meshkov<sup>1</sup>, A. Sorin<sup>1</sup>, and G. Trubnikov<sup>1</sup>

<sup>1</sup>Joint Institute for Nuclear Research, Joliot-Curie, 6, Dubna, Moscow reg., Russian Federation, 141980

**Abstract.** The project NICA (Nuclotron-based Ion Collider fAcility) is aimed to study hot and dense baryonic matter in heavy ion collisions in the energy range up to  $\sqrt{s_{NN}}=11$  GeV, and to study nucleon spin structure in polarized proton and deuteron collisions in the energy range up to  $\sqrt{s}=27$  GeV. The heavy ion program will be performed at the Nuclotron extracted beams with the BM@N (Baryonic Matter at Nuclotron) set-up and with the MPD (MultiPurpose Detector) at the NICA collider with the average luminosity of  $L = 10^{27} \text{ cm}^{-2}\text{s}^{-1}$  (for  $^{197}\text{Au}^{79+}$ ). The spin physics will be studied with the SPD (Spin Physics Detector) at the NICA collider.

### 1 Introduction

The NICA (Nuclotron-based Ion Collider fAcility) project is under realization at the Joint Institute for Nuclear Research (JINR) in Dubna [1–3]. The main goals of the project are study of hot and dense baryonic matter at the extreme conditions in heavy ion collisions, and investigation of nucleon spin structure in the collisions of polarized protons and deuterons. The NICA is an accelerator and experimental complex which includes collider to provide collisions of ions with atomic masses up to gold with energy range  $\sqrt{s_{NN}} = 4 - 11$  GeV for  $\text{Au}^{79+}$ , and polarized protons and deuterons with energy up to  $\sqrt{s}=27$  GeV for protons. This energy range will be extended to cover the lower energy region providing fixed target experiments in the beams extracted from the Nuclotron. The NICA complex comprises two collider experiments, MultiPurpose Detector (MPD) to study heavy ion collisions, and Spin Physics Detector (SPD) to study collisions of polarized particles, and one fixed target experiment – Baryonic Matter at Nuclotron (BM@N).

The physic program in heavy ion collisions is aimed to explore the QCD phase diagram in the region of hot and dense baryonic matter. The NICA energy covers the region of maximum baryonic density in phase transition. The strategy is to perform a detailed energy and system size scan with an emphasis to the production of hadrons and dileptons, event-by-event fluctuations and correlations. This program includes a search for the mixed phase of the quark and hadronic matter formed in heavy-ion collisions as a consequence of a first order phase transition. Existing data on single-particle spectra and mean multiplicities [4] suggest that this transition occurs within the NICA energy range.

The range of collision energies is promising for dilepton studies since the effect of vector meson modifications is expected to be sensitive to the baryon density, while the latter happens to reach the maximum in central Au+Au collisions at NICA [5].

<sup>a</sup>e-mail: kekelidze@jinr.ru

The theory predicts strangeness enhancement in heavy-ion induced interactions (relative to elementary p+p collisions), which might be a signature for the deconfinement phase transition [6]. Taking into account small hadronic cross-sections of multi-strange hyperons, and not as strong as for other hadrons re-scattering effects of hyperons in the dense nuclear matter, nuclear objects with strangeness - hypernuclei [7] can be produced with considerably enhanced rates at the NICA energies [8]. New experimental data of NICA on (anti)hyperon and hypernuclei production will provide a valuable insight into the reaction dynamics and properties of the QCD matter.

The studies in the collider mode will be complemented by a fixed target experiment BM@N in the beams extracted from the Nuclotron at energies up to 6 GeV per nucleon. The BM@N research program on heavy-ion collisions includes [9]: investigation of reaction dynamics and nuclear EOS, study of in-medium properties of hadrons, production of (multi)-strange hyperons at the threshold and search for hypernuclei. Particle yields, ratios, transverse momentum spectra, rapidity and angular distributions, as well as fluctuations and correlations will be studied at BM@N as a function of the collision energy and centrality.

The spin physics program is under development and the corresponding detector SPD is at the design stage. The SPD experiment will provide unique opportunity to study eight Parton Distribution Functions (PDFs) in one experiment and obtain a comprehensive information on the nucleon spin structure at high statistical level with minimum systematic uncertainties. The nucleon spin structure will be studied using the Drell-Yan mechanism exploring 8 intrinsic-transverse-momentum dependent PDFs (new PDFs) at leading twist azimuthal asymmetries with different angular modulations in the hadron and spin azimuthal angles,  $F_h$  and  $F_s$ .

More detailed information on the NICA physics program is available in [10].

## 2 Accelerator complex

The view of the NCA complex is presented in Fig. 1.

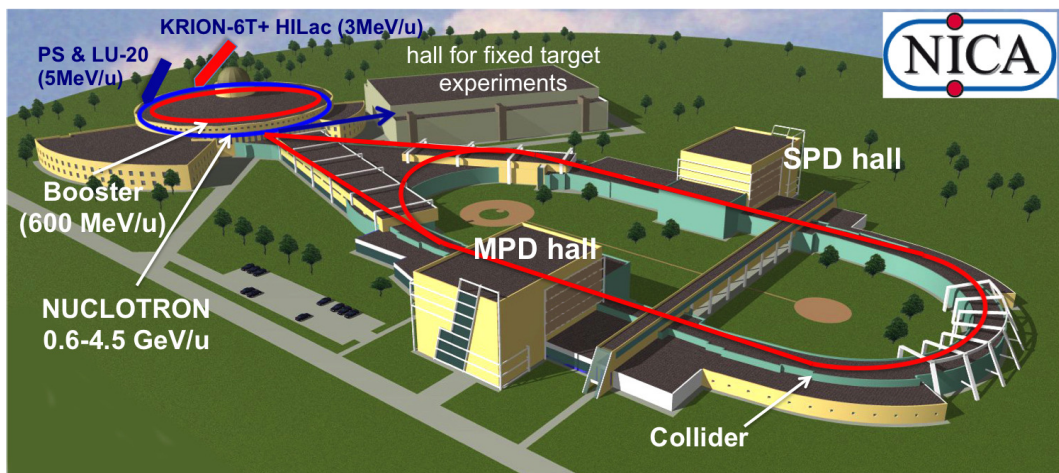


**Figure 1.** The NICA complex: existing facility (blue) and to be constructed one (red)

The existing facility consists of:

- injector comprising set of light ion sources including source of polarized protons and deuterons (PS), and Alvarez-type linac LU-20;
- Nuclotron – superconducting (SC) proton synchrotron with maximum magnetic rigidity of  $45T \cdot m$  and the circumference of 251.52 m providing acceleration of completely stripped  $^{197}\text{Au}^{79+}$  ions up to the experiment energy of 4.5 GeV/u and protons up to the energy of 12.6 GeV;
- area with fixed target experiments.

The new facility to be constructed comprises:

- new injector consisting of ESIS-type ion source that provides  $^{197}\text{Au}^{31+}$  ions of the intensity of  $2 \cdot 10^9$  ions per pulse of about  $7 \mu\text{s}$  duration at possible repetition rate up to 50 Hz, and heavy ion linear accelerator (HILAc) consisting of RFQ and RFQ Drift Tube Linac (RFQ DTL) sections accelerating ions at  $A/q \leq 8$  up to the energy of 3 MeV/u at efficiency not less than 80 %;
- Booster-synchrotron housed in the Synchrophasotron yoke window and consisting of SC magnetic system providing maximum magnetic rigidity of  $25T \cdot m$  at the ring circumference of 215 m, and equipped with electron cooling system that allows to provide cooling of the ion beam up to the energy of 100 MeV/u. The maximum energy of  $^{197}\text{Au}^{31+}$  ions accelerated in the Booster is of 600 MeV/u; stripping foil placed in the transfer line from the Booster to the Nuclotron allows to provide the stripping efficiency at the maximum Booster energy not less than 80 %;
- transfer line transporting the particles from Nuclotron to Collider rings;
- two SC collider rings with maximum magnetic rigidity of  $45T \cdot m$  and the circumference of about 503.4 m equipped with electron and stochastic cooling systems and providing gold-gold collisions at the energy range  $\sqrt{s_{NN}} = 4 - 11$  GeV and p-p collisions at the energy up to  $\sqrt{s} = 27$  GeV.

The NICA collider will provide average luminosity  $L = 10^{27} \text{ cm}^{-2}\text{s}^{-1}$  and  $10^{32} \text{ cm}^{-2}\text{s}^{-1}$  for gold-gold and proton-proton collisions, respectively. To reach such luminosity a special procedure of formation of high intensity ion bunches in the collider is developed. First, the ions accelerated in the injection accelerator chain are stored in the Collider rings with so called “barrier bucket (BB) technique” that allows to reach the required intensity of the beam. Then the beam becomes coasting after switching off the BB RF system and bunched on 22nd harmonics of the harmonic RF. When bunches are compressed sufficiently they are captured in 66th harmonics that forms short and dense bunches. Afterwards, the colliding mode is turned on by the system of the beam orbit correction.

### 3 MPD detector

The Multi Purpose Detector (MPD) is designed as a  $4\pi$  spectrometer capable detecting of charged hadrons, electrons and photons in heavy-ion collisions at high luminosity in the energy range of the NICA collider [11]. The experimental setup (see Fig. 2) will comprise a precise 3D tracking system and a high-performance particle identification (PID) system based on the time-of-flight measurements and calorimetry. The event rate of minimum bias interactions is of about 7 kHz, and the total charge particle multiplicity exceeds 1000 in the most central Au+Au collisions at  $\sqrt{s_{NN}}=11$  GeV. The detector design requires a very low material budget. The whole detector setup (Fig. 2) includes Central Detector (CD) covering pseudorapidity interval  $|\eta| < 2$  and two forward spectrometers (FS-A,B) for  $2 < |\eta| < 3$  (optional). The cross-sectional view of the MPD Central Detector (CD) is shown in Fig. 3. The MPD CD is 9 meters long and 6.6 meters in diameter and will be constructed in two stages. At the first stage (at the end of 2019) MPD will consist of the superconducting solenoid with a flux return yoke, Time-Projection Chamber (TPC), barrel Time-Of-Flight system (TOF), Electromagnetic

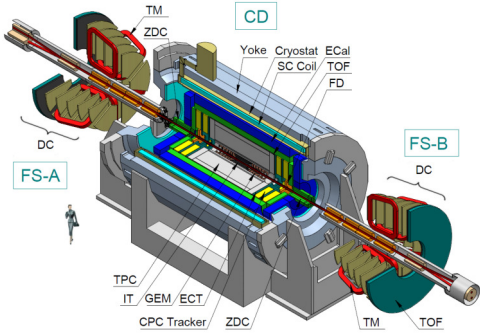


**Figure 2.** MPD setup.

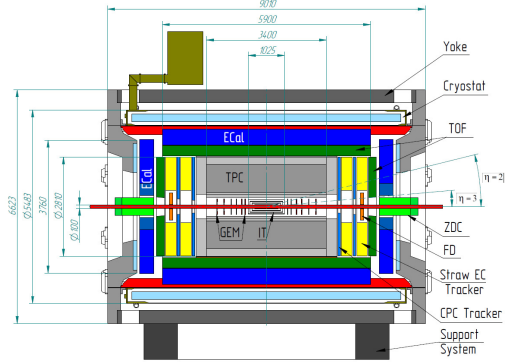


**Figure 3.** The MPD central detector cross-sectional view.

Calorimeter (ECal), Zero-Degree Calorimeter (ZDC) and Fast Forward Detector (FFD). A detailed description of the detector parts can be found in Ref. [12].

The Time-Projection Chamber is the main tracking detector of the MPD and will provide: tracking and particle ID ( $dE/dx$  measurements with a resolution better than 8%) in the pseudo rapidity range  $|\eta| < 1.2$ , momentum resolution for charge particles better than 3% in the transverse momentum range  $0.1 < p_T < 1$  GeV/c and two-track resolution of about 1 cm. The TPC has an inner diameter of 54 cm, an outer diameter of 280 cm, and an overall length along the beam direction of 340 cm. The TPC field cage will be made of composite materials (kevlar and tedlar), with the overall thickness to be less than 5% X0. For precise tracking the relative radial magnetic and electric field components in MPD have not to exceed  $\approx 5.2 \cdot 10^{-4}$ . The TPC readout system at the first stage is based on the Multi-Wire Proportional Chambers (MWPC) with cathode pad readout. The gas mixture of 90% argon and 10% methane (P10) or 90%Ar and 10% CO<sub>2</sub> is supposed to be used. In Fig. 4 a relative momentum resolution ( $\Delta P/P$ ) for charged tracks in the MPD TPC from Monte-Carlo simulations is shown.

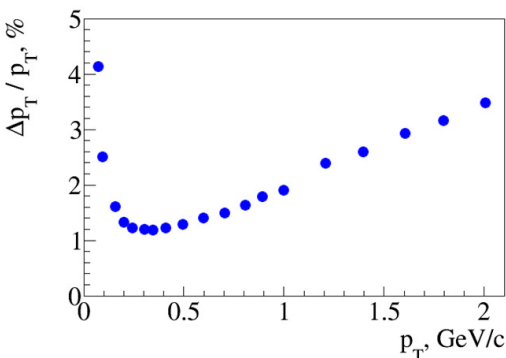


**Figure 4.**  $\Delta P_T/P_T$  as a function of transverse momentum in MPD.

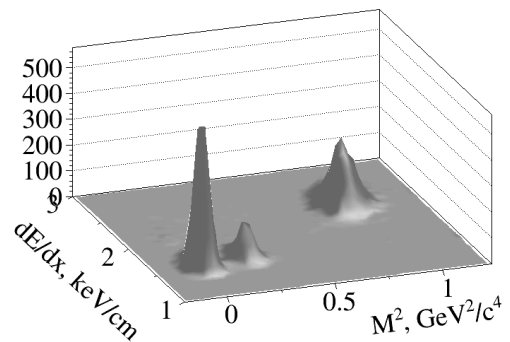


**Figure 5.** A typical distribution of the specific energy loss  $dE/dx$  versus mass-squared for  $\pi^+$ ,  $K^+$ , and protons (from left to right) at  $p = 1$  GeV/c.

Identification of charged hadrons will be achieved by the time-of-flight (TOF) measurements which are complemented by the energy loss ( $dE/dx$ ) information from the TPC (see Fig. 5). The

cylindrical part of the TOF MPD has a full azimuthal and  $|\eta| < 1.2$  coverage. The TOF outer diameter is 3.4 m and the total surface is of about  $53 \text{ m}^2$ . The basic element of the TOF system will be a Multigap Resistive Plate Chamber (MRPC). The TOF electronics will be based on the NINO specific integrated circuit [13] and TDC based on a multihit High Performance ASIC (HPTDC) chip developed at CERN [14]. The detector is segmented in azimuth into 12 sectors of 5.7 m length. Each sector consists of 4 modules and each module comprises 6 MRPCs detectors arranged in 2 layers. The overall TOF geometrical efficiency is above 95% and time resolution is better than 100 ps. It would allow to separate pions from kaons up to  $p_t < 1.5 \text{ GeV}/c$  and identify (anti)protons up to  $p_t \approx 3 \text{ GeV}/c$ . As can be seen from Fig. 5, the basic detector parameters, namely,  $dE/dx$  resolution of  $\sigma_{dE/dx} \approx 8\%$  and TOF resolution of  $\sigma_{TOF} \approx 100 \text{ ps}$  will provide a high degree of selectivity for hadrons at momenta below  $2 \text{ GeV}/c$ .

The primary role of the electromagnetic calorimeter is to measure the spatial position and energy of electrons and photons produced in heavy ion collisions. The electromagnetic calorimeter will be built of towers as basic elements of about  $3 \text{ cm}^2$  cross section. Each lead-scintillator sampling tower contains 250 alternating tiles of Pb (0.275 mm) and plastic scintillator (1.5 mm). A module of 18 radiation length thickness will be  $\approx 40 \text{ cm}$  long. The cells of each tower are optically combined by 9 longitudinally penetrating wavelength shifting fibers for light collection. The light collected by these fibers will be read out by avalanche photodiodes (MAPD) units of  $3 \times 3 \text{ mm}^2$  sensitive area. The towers, mechanically grouped together, make 139 trapezium-shape modules which are combined into 48 detector sectors. The heat-producing electronics will be thus separated from the modules and mounted on the upper parts of sectors.

The FFD detector located at  $\approx 75 \text{ cm}$  on both sides of the interaction point will provide a fast trigger and timing signal for TOF. A FFD module made of 1.5 cm thick quartz Cherenkov radiator optically coupled to a multianode MCP-PMT Planacon, is capable of register high energy photons and relativistic charged particles of velocity  $\beta > 0.69$  with a timing resolution better than 50 ps.

The MPD Zero Degree Calorimeter (ZDC) located in the both sides of MPD at a distance of 3.2 m from the MPD center will be used for classification of events by centrality by measuring the energy of spectators. Each ZDC semi-part consists of identical modules parallelepiped-shaped with a transverse cross-section of  $10 \times 10 \text{ cm}^2$  and a length of 90 cm. Each of ZDC modules consists of 60 lead-scintillator tile "sandwiches" of thickness of 16 and 4 mm for Pb and scintillator, respectively. The sampling ratio of 4:1 will provide the compensation condition. WLS-fibers from each of 6 consecutive scintillator tiles are collected together and viewed by an avalanche photodiode at the end of each module.

## 4 MPD feasibility study

All the Monte-Carlo simulation and feasibility study for MPD were performed in the framework of a dedicated program tool - MPDRoot comprising interfaces to many event generators and Geant as well as detector response simulation and reconstruction algorithms.

The performance of the MPD detector for hyperon measurements was studied for a combination of Time Projection Chamber (TPC) and Time-Of-Flight system (TOF) covering the mid-rapidity region ( $|\eta| < 1.3$ ). A material budget not exceeds 10% of  $X_0$  in the region of interest. A powerful particle ID based on ionization loss ( $dE/dx$ ) measurements in the TPC and time-of-flight information from the TOF, allows one a precise trajectory reconstruction and a reliable separation of particle species.

Hyperons and cascades were reconstructed using the secondary vertex finding technique with an optimized set of topological and track quality cuts as described in [15]. In Fig. 6 are shown invariant mass distributions of  $(p, \pi^-)$ ,  $(\Lambda, \pi^-)$  and  $(\Lambda, K^-)$  pairs from central Au+Au collisions at center-of-mass energy  $\sqrt{s} = 9 \text{ GeV}$ . The estimated yields of particle species for 10 weeks of data taking at the

nominal luminosity are  $\approx 10^7$  and  $\approx 10^6$  for  $\Xi^-$  and  $\Omega^-$ , respectively. The accumulated statistics will allow one to get information on cascade production over a broad region of the QCD phase diagram and a large phase-space of the reaction.

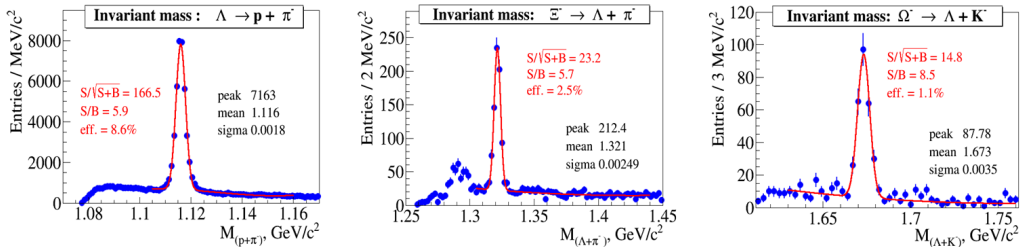


**Figure 6.** Invariant mass of  $p$  and  $\pi^-$  (left),  $\Lambda$  and  $\pi^-$  (center),  $\Lambda$  and  $K^-$  (right) candidates.

A detailed description of the analysis procedure and results of the MPD performance can be found in Ref. [16]. The charged hadrons and dileptons from event generators (UrQMD+Pluto) were transported through the detector setup. A realistic detector response was simulated followed by track reconstruction, TPC-TOF matching and particle identification procedures performed within the MPDRoot framework. Electron identification was achieved by using combined information about the specific energy loss  $dE/dx$  from TPC, time-of-flight from TOF and  $E/p$  information from EMC. The overall hadron rejection factor was achieved to be  $\approx 3200$ .

The background from conversion pairs was eliminated by an extra set of topological and kinematical cuts. Fig. 7 presents a spectrum of reconstructed low-mass dielectrons after background rejection (dots), and a spectrum of true dielectrons from the event generator (line).  $S/B$  ratio in mass region  $0.2 < M_{e^+e^-} < 1.2 \text{ GeV}/c^2$  was estimated to be of about 10% which indicate MPD performance at the level of best published experimental results.

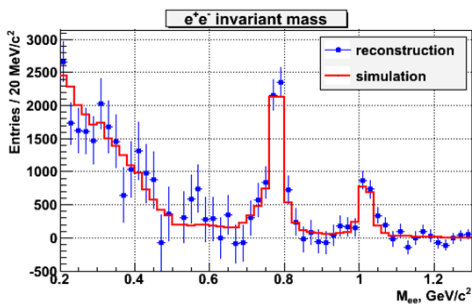


**Figure 7.** Invariant mass of dileptons after background subtraction.

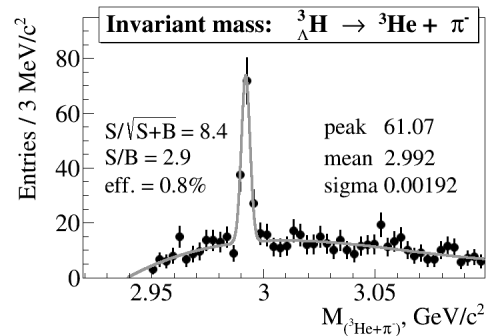


**Figure 8.** Invariant mass of  ${}^3\text{He}$  and  $\pi^-$  candidates (MPD).

$5 \cdot 10^5$  events from the DCM-QGSM event generator corresponding  $\approx 30$  minutes of data taking time at NICA were used to study of MPD capability for reconstruction of hypertritons. The event reconstruction, particle ID and secondary vertex finding are described in [15]. The obtained invariant

mass spectra of helium-3 and  $\pi^-$  candidates is shown in Fig. 8. This result demonstrates a good sensitivity of the MPD setup for hypernuclei detection. About  $10^5$  hypertritons will be detected in a week of data taking with a typical event rate of 7 kHz for the design NICA luminosity of  $10^{27}\text{cm}^{-2}\text{s}^{-1}$ . Thus, a detailed study of the production mechanism of single hypernuclei as well as an observation of double hypernuclei at NICA look feasible.

## 5 BM@N experiment

The BM@N) experiment will start in 2017 in a beam extracted from the Nuclotron. The Nuclotron will provide variety of beams from protons to gold ions with the kinetic energy from 1 to 6 GeV per nucleon. The ion beams of masses up to Xe will be available by the end of 2017. The gold beam with intensity  $10^7/s$  is planned in 2019.

A sketch of the BM@N set-up is shown in Fig. 9. It combines high precision track measurements

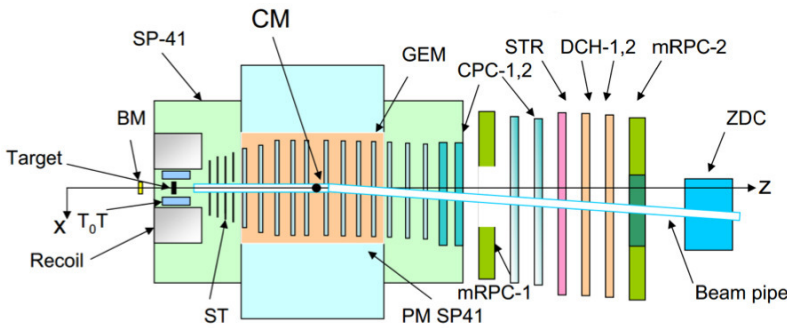


**Figure 9.** The BM@N experimental set-up.

with time-of-flight information for particle identification and total energy measurements for the analysis of the collision centrality. The charged track momentum and multiplicity will be measured with the set of 12 two-coordinate planes of GEM (Gaseous Electron Multipliers) detectors located downstream of the target inside the analyzing magnet complemented by drift and straw tube chambers situated outside the magnetic field. At the second stage of the BM@N experiment, at least 4 planes of two-coordinate silicon strip detectors will be installed between the GEM tracker and the target. The design parameters of the time-of-flight detectors based on multi-gap Resistive Plate Chambers (mRPC-1,2) with a strip read-out will allow to discriminate between hadrons ( $\pi$ ,  $K$ ,  $p$ ) as well as light nuclei with the momentum up to a few GeV/c. The Zero Degree Calorimeter (ZDC) is designed for the analysis of the collision centrality by measuring the energy of forward going particles. The T0 detector, partially covering the backward hemisphere around the target, is planned to trigger on central heavy ion collisions and provide a start signal for the mRPC-1,2.

The detector set-up was optimized for the measurement of strange hyperons and hyper-nuclei in central Au+Au collisions. In Figures 10 and 11 are shown invariant mass of ( $\Lambda$ ,  $\pi^-$ ) and ( ${}^3\text{He}$ ,  $\pi^-$ ) candidates, respectively, reconstructed with the GEM tracker from central Au+Au collisions at the beam kinetic energy of 4.5A GeV. The obtained results indicate a reasonable reconstruction capability for strange hyperons produced in high multiplicity central Au+Au collisions. The reconstructed signals of  $\Xi^-$ -hyperon and hyper-triton correspond to 0.9M and 2M of central collisions, respectively. The expected statistics of  $\Xi^-$ -hyperons and hypertritons for a month of the BM@N operation are expected

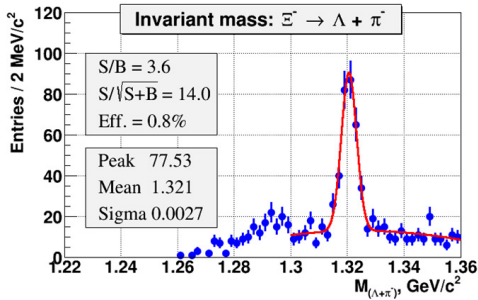


**Figure 10.** Invariant mass of  $\Lambda$  and  $\pi^-$ .

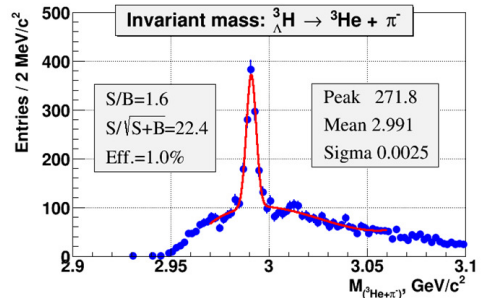


**Figure 11.** Invariant mass of  ${}^3\text{He}$  and  $\pi^-$  candidates.

to be of 2.7M and 4M, respectively. This statistics is sufficient to perform studies of strange hyperon and hyper-nuclei production by measuring their transverse momentum spectra, rapidity and angular distributions.

## 6 Summary

Design and construction of the the new facility at the JINR is in progress. The NICA will provide competitive research program complementary to those of BNL, CERN and that planned at FAIR.

## References

- [1] G. Trubnikov, A. Kovalenko, V. Kekelidze, I. Meshkov, R. Lednicky, A. Sissakian, A. Sorin, PoS (ICHEP 2010) 523.
- [2] G. Trubnikov, N. Agapov, V.Kekelidze, A. Kovalenko, V. Matveev, I.Meshkov, R. Lednicky, A. Sorin, PoS 36th International Conference of High Energy Physics (ICHEP2012), July 4-11, Melbourne, Australia.
- [3] V.Kekelidze, A. Kovalenko, R. Lednicky, V. Matveev, I.Meshkov, A. Sorin, G. Trubnikov, 37th International Conference on High Energy Physics, ICHEP 2014, Valencia, Spain, 2 Jul 2014 - 9 Jul 2014 Nuclear physics B Proceedings supplements (2014).
- [4] C. Alt et al, *Phys. Rev. C* **77**, 024903 (2008).
- [5] J. Randrup and J. Cleymans, *Phys. Rev. C* **74**, 047901 (2006).
- [6] J. Rafelski and B. Muller, *Phys. Rev. Lett.* **48**, 1066 (1982).
- [7] A.K. Kermann and M.S. Weiss, *Phys. Rev. C* **8**, 408 (1973).
- [8] J. Steinheimer et al., *Phys. Lett. B* **714**, 85 (2012).
- [9] BMN Conceptual Design Report. [http://nica.jinr.ru/files/BMN/BMN\\_CDR.pdf](http://nica.jinr.ru/files/BMN/BMN_CDR.pdf).
- [10] NICA White Paper, <http://nica.jinr.ru>, free access
- [11] K.U. Abraamyan et al., *Nucl. Instrum. Meth. A* **628**, 99 (2011).
- [12] MPD Conceptual Design Report. [http://nica.jinr.ru/files/CDR\\_MPD/MPD\\_CDR\\_en.pdf](http://nica.jinr.ru/files/CDR_MPD/MPD_CDR_en.pdf).
- [13] F. Anghinolfi et al., *Nucl. Instr. Meth. A* **533**, 183-187 (2004).
- [14] J. Christiansen, HPTDC V 1.3, March 2004, [http://tdc.web.cern.ch/tdc/hptdc/docs/hptdc \(manual, ver2.2.pdf\)](http://tdc.web.cern.ch/tdc/hptdc/docs/hptdc(manual, ver2.2.pdf)).
- [15] M. Ilieva et al. Proceedings of SQM-2015 (to be published).
- [16] A. Zinchenko et al. Proceedings of SQM-2015 (to be published).